



MSAS – Final project

Giulio Pacifici, Lorenzo Porcelli, Giacomo Velo

1 The real system

The **Gravity Field and Steady-State Ocean Circulation Explorer (GOCE)** (**Figure 1**) was a satellite developed by ESA and conceived to map the Earth's gravity field.

In order to detect gravitational gradients, the spacecraft was equipped with a highly accurate gravity gradiometer, which consisted of three pairs of accelerometers placed along 3 orthogonal axes. The GOCE was placed on a very low Earth orbit (altitude of 240-280 km [2]) so that high accuracy measurements could be collected. The strong decay of the orbit due to atmospheric drag was continuously compensated by the Drag-Free and Attitude Control System (*DFACS*) [3], in which dual Kaufman-type ion thrusters were employed. The errors in gravity gradient measurements caused by non-gravitational forces were so limited and the path of the spacecraft was regularly restored as closely as possible to a purely inertial trajectory.



Figure 1: Artist's view of GOCE. [1]

2 The physical model

The *DFAC* system is modeled considering only the translational dynamics in the velocity direction, its physical model includes a capacitive MEMS type accelerometer [4], a flow control valve, and a single ion thruster.

The accelerometer is assumed to be constantly aligned with the direction of the satellite's velocity vector (**Figure 2**). A proof mass of negligible thickness is electrically suspended between two fixed plates. A series of two capacitors C_1 and C_2 is formed since charges are accumulating on its surface, the values of capacitance vary with the position of the mass. The latter is altered by the thrust and the drag acting on the satellite. The output voltage V_{out} of the electrical circuit is a measure of the displacement from the equilibrium position (the mid-line) and is passed to the circuit of the flow control valve. A PD controller generates a control voltage V_c based on the value of V_{out} that tends to restore the central position of the proof mass. All the electrical components on the circuit are assumed to be ideal and no resistive or inductive effect is considered.

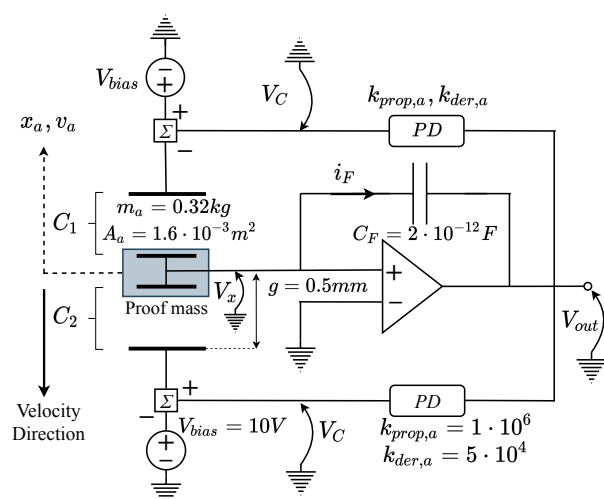


Figure 2: Physical model of the accelerometer.

The flow control valve sketched in **Figure 3a** is modeled as a proportional solenoid valve in which the output voltage of the accelerometer is processed by a PI controller that regulates the current flowing in the inductor. The dynamics of the electrical circuit of the solenoid valve [6] is neglected and the electromagnetic force exerted on the spool is assumed to be proportional to the current in the inductor. The spool is connected to an ideal spring and a viscous force proportional to its velocity acts on it.

The xenon flows in a duct from the tank to the thruster, it is assumed to be a homoentropic ideal gas with adiabatic constant γ that reaches the sonic condition in the throat section. The area of the latter is determined by the position of the spool.

Concerning the ion thruster, it is assumed that its dynamic response is negligible, the acceleration voltage is constant and the ionization of the gas is complete. Thus the thruster is modeled as a single block that generates a value of thrust that depends on the xenon mass flow rate (**Figure 3b**), since the static contribution due to the exit pressure is neglected. The variation of mass of the satellite due to the expulsion of the gas is not taken into account since it has a negligible impact on the system response.

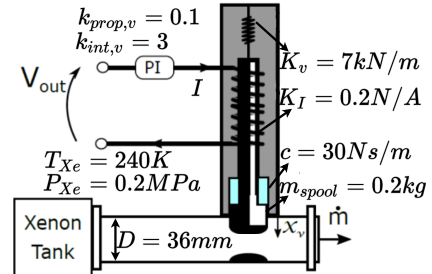
The attitude dynamics of the spacecraft is neglected. The orbital dynamics is modeled as a perturbed two body problem in which the drag, the $J2$ effect and the thrust are the perturbing accelerations. Other perturbations, as solar radiation pressure and other bodies' attractions, are not considered, since they have a smaller effect on the orbit if compared to the other disturbances. The drag acceleration is computed assuming a constant value of the ballistic coefficient of the spacecraft and a rotating atmosphere. The model used for the atmospheric density is the *CIRA72* [7] (*COSPAR* international reference atmosphere), a piece-wise exponential model of the density as a function of the altitude that is computed considering Earth as an oblate spheroid.

Noise is neglected in the physical model, while uncertainties on the numerical values of the parameters of the system are considered in a statistical analysis.

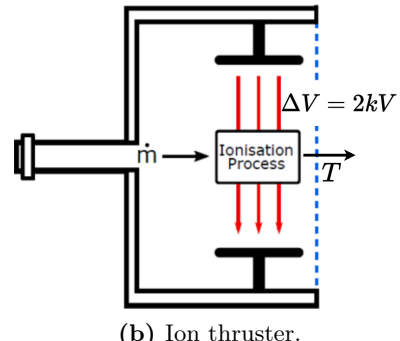
3 The mathematical model

The orbital motion of GOCE is modeled through the Gauss planetary equations (*GPE*), which define the variations of the Keplerian elements (a , e , i , Ω , ω , θ) due to the perturbations (**Equation 1**).

$$\begin{cases} \dot{a} = 2a \frac{v}{\mu_{\oplus}} a_t \\ \dot{e} = \frac{1}{v} (2(e + \cos \theta)a_t - \frac{r}{a} \sin \theta a_n) \\ \dot{i} = r \frac{\cos(\omega+\theta)}{h} a_h \\ \dot{\Omega} = r \frac{\sin(\omega+\theta)}{h \sin i} a_h \\ \dot{\omega} = \frac{1}{ev} [2 \sin \theta a_t + (2e + \frac{r}{a} \cos \theta) a_n] - r \sin(\omega + \theta) \frac{\cos i}{h \sin i} a_h \\ \dot{\theta} = \frac{h}{r^2} - \frac{1}{ev} (2 \sin \theta a_t + (2e + \frac{r}{a} \cos \theta) a_n) \end{cases} \quad (1)$$



(a) Flow control valve.



(b) Ion thruster.

Figure 3: Physical models of the subsystems of the DFACS. [5]



μ_{\oplus} is the gravitational parameter of the Earth, $r = \|\vec{r} = [x, y, z]^T\|$ is the norm of the position vector in an Earth-centered equatorial reference frame $\{\hat{i}, \hat{j}, \hat{k}\}$, $v = \|\vec{v}\|$ is the norm of the velocity vector in the same frame and $h = \|\vec{h}\| = \|\vec{r} \times \vec{v}\|$ is the norm of the specific angular momentum. The total perturbation $\vec{a} = [a_t, a_n, a_h]^T$ is expressed in the $\{\hat{t}, \hat{n}, \hat{h}\}$ orbit frame (tangential - normal - out of plane) and includes the contributions of J2, drag and thrust. The singularity conditions of the right hand side ($i = 0^\circ$ or $e = 0$) are never met in the simulation.

The perturbing accelerations due to J2 and to the drag are computed in the $\{\hat{i}, \hat{j}, \hat{k}\}$ frame as (**Equation 2**):

$$\begin{cases} \vec{a}_{J2} = \frac{3J_2\mu_{\oplus}R_E}{2r^4} \left[\frac{x}{r} \left(\frac{5z^2}{r^2} - 1 \right) \hat{i} + \frac{y}{r} \left(\frac{5z^2}{r^2} - 1 \right) \hat{j} + \frac{z}{r} \left(\frac{5z^2}{r^2} - 3 \right) \hat{k} \right] \\ \vec{a}_D = \frac{\vec{D}}{m_{GOCE}} = -\frac{1}{2} \frac{1}{\beta} \rho v_{rel}^2 \frac{\vec{v}_{rel}}{\|\vec{v}_{rel}\|} \end{cases} \quad (2)$$

R_E is the equatorial radius of the Earth. The mass of the spacecraft m_{GOCE} is assumed to be equal to 300 kg and its ballistic coefficient is $\beta = m_{GOCE}/(A_{front} \cdot CD) = 300\text{ kg/m}^2$. ρ is the atmospheric density and $\vec{v}_{rel} = \vec{v} - \vec{\omega}_{\oplus} \times \vec{r}$ is the relative velocity of the spacecraft with respect to the Earth's atmosphere (whose angular velocity is $\vec{\omega}_{\oplus}$). These accelerations must be rotated to be expressed in the $\{\hat{t}, \hat{n}, \hat{h}\}$ frame.

The acceleration due to the ion propulsion is always considered to be parallel to the direction of the local velocity \hat{t} and is computed as following (**Equation 3**):

$$\begin{cases} a_T = \frac{T}{m_{GOCE}} = \frac{1}{m_{GOCE}} \dot{m} v_e \\ \dot{m} = \frac{P_{Xe} A_O}{(1 + \frac{\gamma-1}{2})^{2(\gamma-1)}} \sqrt{\frac{\gamma}{RT_{Xe}}} \\ v_e = \sqrt{2 \frac{e^+ \Delta V}{M_{Xe}^+}} \end{cases} \quad (3)$$

The exit velocity of the flow depends on the voltage of the grid ΔV , on the electric charge of the xenon ion $e^+ = |e^-|$ and on its mass M_{Xe}^+ . The mass flow rate is related instead to the pressure P_{Xe} and temperature T_{Xe} . R is the gas constant of xenon. The variable term in the thrust is A_O , which is the area of the orifice defined by the position of the spool in the flow control valve (indicated as x_v). It might be expressed as (**Equation 4**):

$$A_O = \frac{D^2}{8} (\alpha - \sin \alpha) \quad (4)$$

where $\alpha = 2 \arccos(1 - 2z)$ and $z = 1 - x_v/D$. The diameter of the duct of the valve is D . The area of the orifice is null when $z = 0$ and is maximum when $z = 1$.

The dynamics of the flow control valve is built up considering the equation of motion of the spool, which has mass m_{spool} (**Equation 5**). The constant of the spring is K_v , the friction coefficient is c and the electro-mechanical constant is K_I . x_0 is the rest position of the spring.

$$\begin{cases} \dot{x}_v = v_v \\ \dot{v}_v = \frac{1}{m_{spool}} [K_v(x_0 - x_v) - c v_v - K_I I] \\ I = k_{prop,v} V_{out} + k_{int,v} \mathcal{I}_{V_{out}}; \quad \text{with: } \mathcal{I}_{V_{out}} = \int_0^t V_{out} d\tau \end{cases} \quad (5)$$

The mathematical model of the accelerometer includes electrical and mechanical dynamics (**Equation 6**):

$$\begin{cases} \dot{x}_a = v_a \\ \dot{v}_a = \frac{1}{m_a} [-F_1 + F_2 + a_{res}]; \quad \text{with: } a_{res} = a_T + \vec{a}_D \cdot \hat{t} \\ F_1 = \frac{1}{2} C_1 \frac{\Delta V_1^2}{g-x_a}; \quad F_2 = \frac{1}{2} C_2 \frac{\Delta V_2^2}{g+x_a}; \quad \text{with: } C_1 = \frac{\epsilon A_a}{g-x_a}; \quad C_2 = \frac{\epsilon A_a}{g+x_a} \\ \Delta V_1 = V_{bias} - V_c - \frac{1}{2} V_x; \quad \Delta V_2 = V_{bias} + V_c + \frac{1}{2} V_x; \quad \text{with: } V_x = \frac{x_a}{g} V_{bias} \end{cases} \quad (6)$$



a_{res} is the residual acceleration of GOCE with respect to a drag and thrust-free orbit. F_1 and F_2 are the repulsive electrostatic forces exerted by the external armatures on the seismic mass m_a due to the voltage drops ΔV_1 and ΔV_2 . The capacitance of the capacitors formed by the mass and the fixed armatures (C_1 and C_2) is varying with the position x_a and is related to the gap g . ϵ is the electric permittivity of vacuum and A_a is the cross-sectional area of the mass. The control voltage V_c depends on the output voltage through the proportional and derivative constants (**Equation 7**).

$$\begin{cases} V_c = k_{prop,a} V_{out} + k_{der,a} \dot{V}_{out} \\ \dot{V}_{out} = -\frac{i_F}{C_F} \\ i_F = \frac{dQ_{1,2}}{dt} = \frac{d(C_1 - C_2)}{dt} V_{bias} = \frac{d(C_1 - C_2)}{dx_a} \dot{x}_a V_{bias} \end{cases} \quad (7)$$

The fully coupled dynamics of the three sub-systems of the DFACS (accelerometer, flow control valve, ion thruster) can be related to the orbital dynamics by introducing a state vector:

$$\vec{x}(t) = [\mathcal{I}_{V_{out}}, x_v, v_v, x_a, v_a, V_{out}, a, e, i, \Omega, \omega, \theta]^T$$

and rewriting **Equation 5**, **Equation 6** and **Equation 1** to get an expression in the form $\dot{\vec{x}}(t) = \vec{f}(\vec{x}(t))$, where the right hand side will be the input for the numerical solver. The expression of $\vec{f}(\vec{x}(t))$ is highly non-linear.

The initial state for the system is taken as:

$$\vec{x}_0 = \vec{x}(t_0) = [0 \text{ V} \cdot s, x_v(t_0), 0 \text{ m/s}, 0 \text{ m}, 0 \text{ m/s}, 0 \text{ V}, 6663.04 \text{ km}, 0.0045, 90^\circ, 0^\circ, 0^\circ, 0^\circ]^T$$

$x_v(t_0)$ is computed as the value that guarantees a null residual acceleration of the spacecraft at $t_0 = 0 \text{ s}$, x_0 is set as $x_v(t_0)$.

The dynamics of the DFACS sub-system (de-coupled from the orbital dynamics) is linearized about the initial condition, the latter represents an equilibrium condition for the six state equations related to the dynamics of the DFACS. The eigenvalues of the resulting linear system are:

$$\lambda_i = \{0, -4.5 \cdot 10^{-4}, -2 \cdot 10^1, -7.5 \cdot 10^1 \pm 1.7 \cdot 10^2 i, -1 \cdot 10^5\}$$

The sub-system has a null eigenvalue, all the other eigenvalues have negative real part; thus the sub-system is simply stable.

4 Numerical integration

The analysis performed in section 3 is useful to properly select a numerical integration scheme. The system is clearly stiff, due to the different orders of magnitude of the eigenvalues λ_i : this result was expected since dynamics of various nature are interacting. The problem is then requiring an *A-stable* or similar integration scheme.

The team chose to employ MATLAB built-in stiff integrators.

Different runs were performed with `ode23s`, `ode23t`, `ode23tb` and `ode15s`, which was the ultimate selection: it managed to provide a comparable solution with respect to the other solvers (in terms of overall behaviour and accuracy) but required a significantly lower computational time (independently of the tolerances). **Table 1** reports reference values of the computational time when integrating $\vec{f}(\vec{x})$ over one orbit with $\text{RelTol} = 1e-8$, $\text{AbsTol} = 1e-8$.

`ode15s` is a variable-step, variable-order solver based on the multi-step backward differentiation formulas (BDFs) and on numerical differentiation formulas (NDFs) of orders 1 to 5. NDFs are a modification of BDFs with

Table 1: Comp. time required by the integrators.

Integrator	Time [s]
<code>ode15s</code>	$8 \cdot 10^{-2}$
<code>ode23s</code>	3
<code>ode23t</code>	$3 \cdot 10^{-1}$
<code>ode23tb</code>	$5 \cdot 10^{-1}$

improved accuracy but poorer A-stability at high orders [8]. The stability region of the BDFs [9] is reported in **Figure 4** along with the angles of A-stability α_0 . **Table 2** compares the values of α_0 for NDFs and BDFs of different orders.

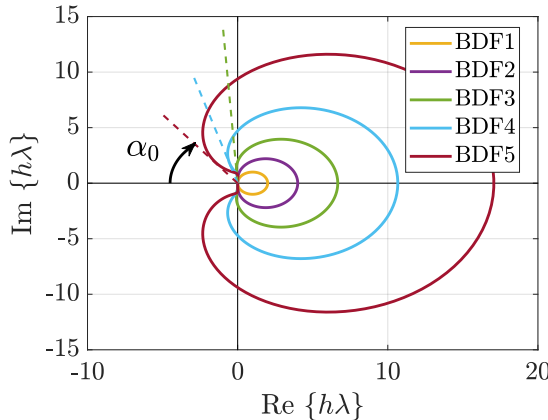


Figure 4: Stability region of BDFs integration schemes (exterior of curves).

The computational time required by `ode15s` to integrate $\vec{f}(\vec{x})$ over one orbit is depicted in **Figure 5**. The plot shows the variation of the time with respect to the relative tolerance for different values of the absolute tolerance. The tolerances for the integration are dynamically changed to globally optimize the computational time of the code. When the simulation is burdened with multiple integrations (e.g. for sensitivity analysis, for optimization) the tolerances are set as $\text{AbsTol} = 1\text{e-}11$, $\text{RelTol} = 1\text{e-}8$. When only plain simulations are needed, the accuracy is improved by selecting $\text{AbsTol} = 1\text{e-}14$, $\text{RelTol} = 1\text{e-}10$. The order and the step size of the integration are automatically chosen by `ode15s` to fulfil the accuracy requirements.

Table 2: A-stability angles of the schemes employed by `ode15s` [8]

Order	α_0 (BDF)	α_0 (NDF)
1	90°	90°
2	90°	90°
3	86°	80°
4	73°	66°
5	51°	51°

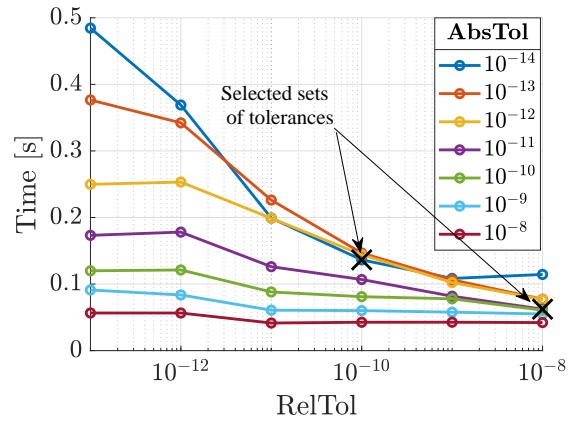


Figure 5: Computational time of `ode15s` for different sets of tolerances (reference values).

5 The simulation framework

A block diagram of the system is depicted in **Figure 6**. Such scheme is used to perform every integration during the overall simulation.

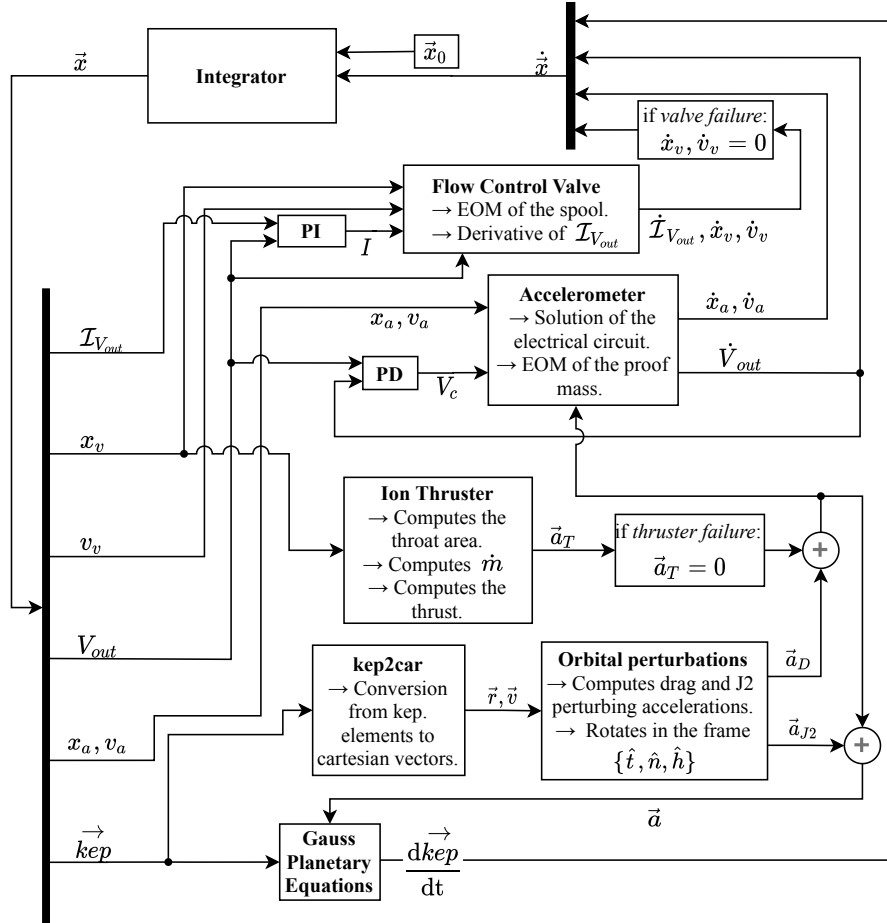


Figure 6: System's block diagram.

6 System response

The system response in nominal conditions is represented in **Figure 7** for a time span of ten orbital periods ($\approx 5.4 \cdot 10^4 s$). It is glaring in **Figure 7e** that the control system is working properly: the residual acceleration oscillates with a lower amplitude than the sole drag (**Figure 7f**) and has a mean value closer to zero.

Figure 8 shows the system response in off-nominal conditions. Two different types of failures are simulated, both affecting the system for a time duration of 2 orbital periods:

- *Thruster failure*: no thrust is produced starting from $t = 1 \cdot 10^3 s$.
- *Valve failure*: the spool is blocked starting from $t = 3.7 \cdot 10^4 s$.

A statistical analysis is performed to retrieve the behaviour of the residual acceleration when uncertainties are introduced on some parameters of the system. The variables listed in **Table 3** are assumed to vary according to a normal distribution centered at their respective nominal value, the values of the standard deviations are reported. Several simulations are performed evaluating the system response during two orbits with a fixed time step of 10s, the random variables change in each simulation according to the normal distribution. The mean value and

the standard deviation $\sigma(t)$ of the residual acceleration at each time step is determined and the envelope in **Figure 9** is computed.

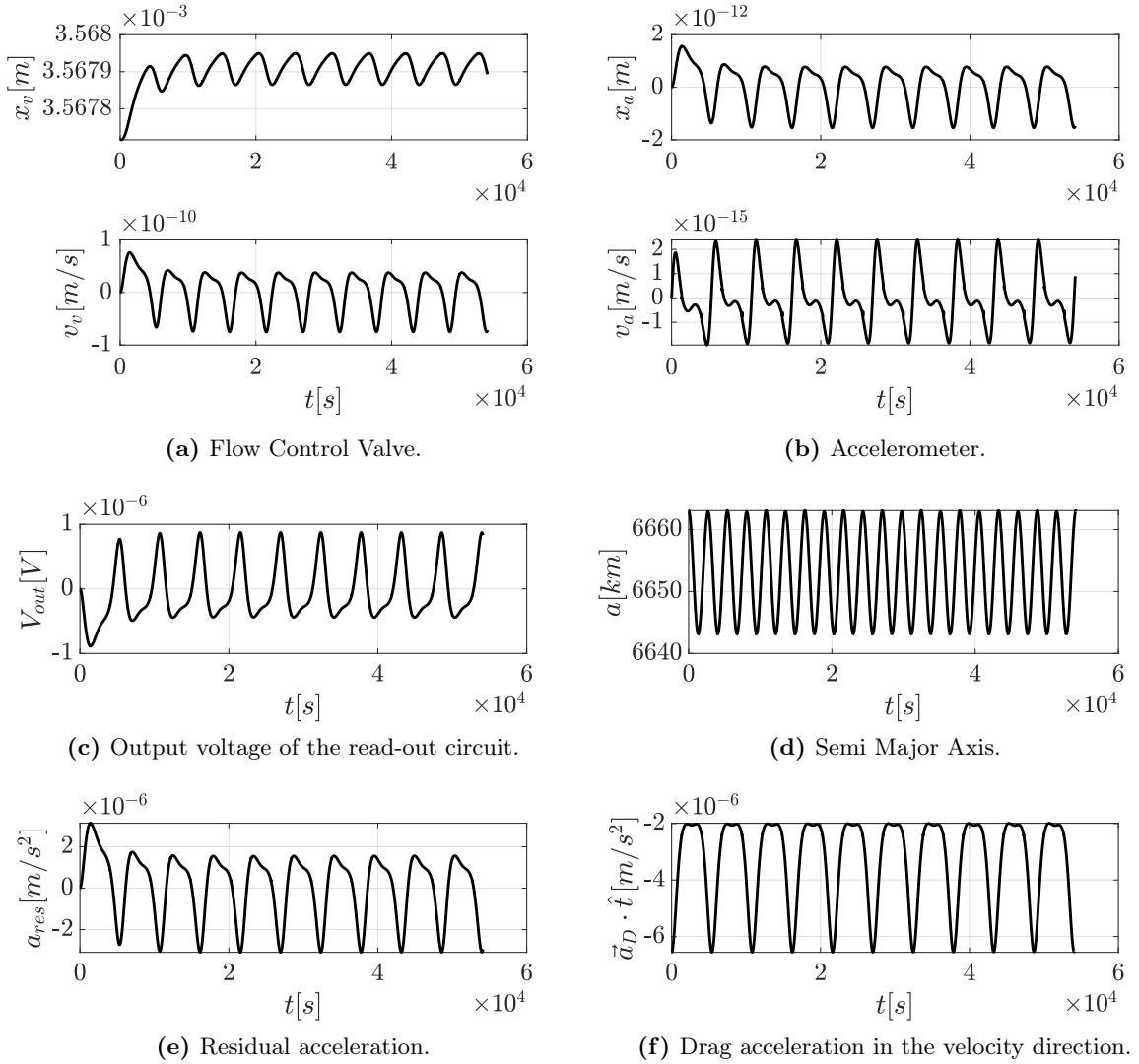


Figure 7: System response in nominal conditions.

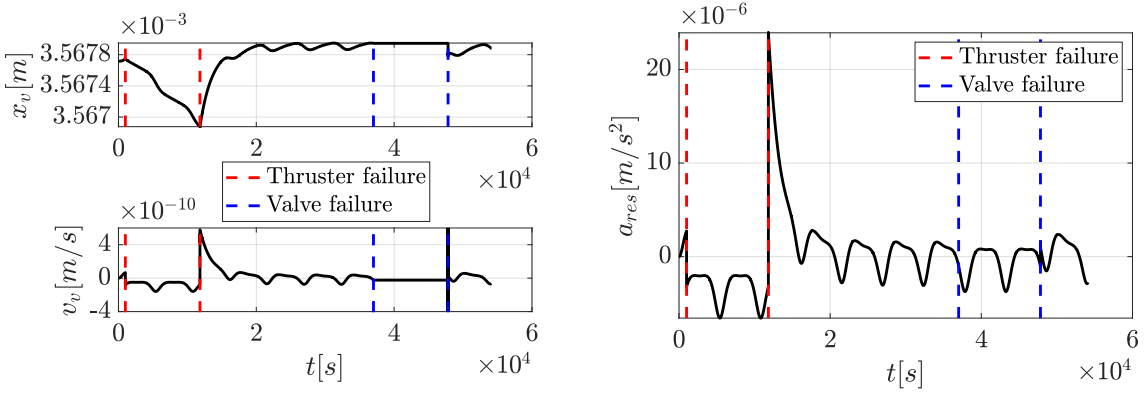


Figure 8: Off-nominal conditions: thrust and control valve failures.

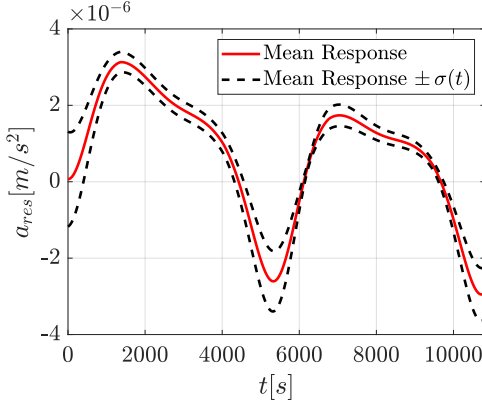


Figure 9: Envelope of the residual acceleration considering uncertainties.

Table 3: Standard Deviations of the uncertain variables (percentage of the nominal values).

Variable	Standard Deviation
CD	20 %
m_{GOCE}	10 %
m_a	10 %
c	20 %
m_{spool}	10 %
K_I	10 %
T_{Xe}	5 %

7 System optimization

The optimization is intended as a fine tuning of some parameters of the system. It is performed selecting a cost function $J = \sqrt{\sum_k a_{res,k}^2}$, where $a_{res,k}$ is the residual acceleration of GOCE evaluated at the k -th instant of an equispaced time array.

The analysis is executed on the controllers' gains, namely: $k_{prop,a}$, $k_{der,a}$, $k_{prop,v}$ and $k_{int,v}$. The optimization is carried out with the MATLAB function fmincon. The cost function J is computed over one orbital period with a sampling frequency of 1Hz. The values of the optimization variables differ by several orders of magnitude, normalization is applied to improve the performances of the optimization algorithm. Lower and upper boundaries for the optimization variables are reported in **Table 4**, the optimal solution found is reported in **Table 5**. In **Figure 10** a comparison between the nominal and the optimized responses is represented for a time span of two orbits. In contrast to the initial system, the optimized solution does not have an initial transient, oscillates with a lower amplitude and has a mean value closer to zero. It is then safe to state that this optimization process has provided a satisfactory result.

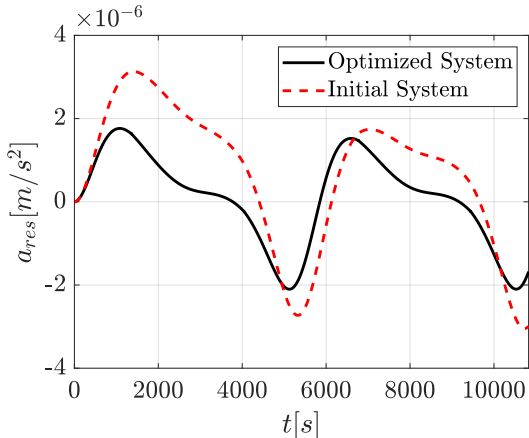


Figure 10: Comparison between initial and optimized responses.

Table 4: Variables' upper and lower boundaries.

Variable	L.B.	U.B.
$k_{prop,a}$	$5 \cdot 10^5$	$2 \cdot 10^6$
$k_{der,a}$	$2.5 \cdot 10^4$	$1 \cdot 10^5$
$k_{prop,v}$	0.05	0.2
$k_{int,v}$	1.5	6

Table 5: Optimized variables.

Variable	Initial Value	Optimized Value
$k_{prop,a}$	$1 \cdot 10^6$	$5 \cdot 10^5$
$k_{der,a}$	$5 \cdot 10^4$	$6.11 \cdot 10^4$
$k_{prop,v}$	0.1	0.15
$k_{int,v}$	3	6



References

- [1] ESA. *GOCE - l'esploratore del campo gravitazionale dell'ESA*. URL: https://www.esa.int/kids/it/imparare/Terra/Il_mondo_marino/GOCE_-_l_esploratore_del_campo_gravitazionale_dell_ESA (visited on 12/02/2020).
- [2] ESA. *GOCE (Gravity field and steady-state Ocean Circulation Explorer)*. URL: <https://earth.esa.int/web/eoportal/satellite-missions/g/goce> (visited on 12/02/2020).
- [3] E. Canuto and L. Massotti. “All-propulsion design of the drag-free and attitude control of the European satellite GOCE”. In: *Acta Astronautica* 64.2 (2009), pp. 325–344. DOI: <https://doi.org/10.1016/j.actaastro.2008.07.017>.
- [4] D. E. Serrano. “Design and analysis of MEMS accelerometers”. In: *IEEE Sensors*. 2013.
- [5] F. Topputto, V. Franzese, and C. Giordano. *Lecture notes for the course "Modeling and simulation of aerospace systems"*. Politecnico di Milano, 2020.
- [6] N. D. Vaughan and J. B. Gamble. “The Modeling and Simulation of a Proportional Solenoid Valve”. In: *Journal of Dynamic Systems, Measurement, and Control* 118.1 (Mar. 1996), pp. 120–125. DOI: 10.1115/1.2801131. eprint: https://asmedigitalcollection.asme.org/dynamicsystems/article-pdf/118/1/120/5595218/120_1.pdf.
- [7] C. C. for the COSPAR International Reference Atmosphere. *CIRA 1972: COSPAR International Reference Atmosphere 1972*. Akademie-Verlag, 1972.
- [8] L. Shampine and M. Reichelt. “The MATLAB ODE suite”. In: *SIAM Journal on Scientific Computing* 18 (May 1997). DOI: 10.1137/S1064827594276424.
- [9] N. Trefethen. *Stability Regions of ODE Formulas*. Feb. 2011. URL: <https://www.mathworks.com/matlabcentral/mlc-downloads/downloads/submissions/23972/versions/22/previews/chebfun/examples/ode/html/Regions.html> (visited on 12/02/2020).